

Giant radio galaxy DA 240 group: content and environment

R. Chen¹, B. Peng^{1,2}, R. G. Strom^{3,4,5,6}, J. Wei¹, and Y. Zhao¹

¹ National Astronomical Observatories, Chinese Academy of Sciences, Beijing 100012, PR China
e-mail: spiritrong@gmail.com

² Joint Laboratory for Radio Astronomy Technology, Datun Road A20, Beijing 100012, PR China

³ Netherlands Institute for Radio Astronomy (ASTRON), Postbus 2, 7990 AA Dwingeloo, The Netherlands

⁴ Astronomical Institute “Anton Pannekoek”, Faculty of Science, University of Amsterdam, The Netherlands

⁵ Centre for Astronomy, James Cook University, Townsville QLD 4811, Australia

⁶ Department of Physics, National University of Singapore, 2 Science Drive 3, Singapore 117542, Singapore

Received 16 April 2010 / Accepted 21 February 2011

ABSTRACT

Context. There is a group of about twenty galaxies around the giant radio galaxy (GRG) DA 240 which we are studying to investigate the environment of the radio source. We have noted that 11 members are aligned with the radio emission (Peng et al. 2004, A&A, 415, 487). The alignment occurs within a small angle similar to the width of the GRG radio lobes, and there may be some physical causal relationship. After finishing observations of the four candidates not included in Paper I, we have completed our study of the brighter members of the sample of galaxies around DA 240.

Aims. We aim to see if more galaxies have similar redshifts to the host galaxy of DA 240, to confirm the galaxy grouping and further study their distribution.

Methods. Spectra of the four candidate galaxies were obtained with the 2.16 m spectroscopic telescope at XingLong observing station of the NAOC, and the galaxies' positions were established with respect to the radio emission. We have discovered two more members associated with the group of galaxies around DA 240. In addition, the work of other researchers provides one other new member.

Results. The number of confirmed galaxies associated with the DA 240 group has increased by almost a quarter to 20. There are now 14 galaxies (including the host) lying along the major axis of the radio source. We further consider the relationship of the group to adjacent galaxy associations, noting that it may form a binary pair with the slightly closer UGC 3957 group. They both lie on the periphery of the much more substantial cluster, Abell 576.

Key words. galaxies: active – galaxies: individual: DA 240 – galaxies: ISM – galaxies: distances and redshifts – techniques: spectroscopic – ISM: jets and outflows

1. Introduction

Giant radio galaxies (GRGs) are defined as a class with a projected linear size ≥ 1 Mpc (e.g. Klein et al. 1994, for $H_0 = 75 \text{ km s}^{-1} \text{ Mpc}^{-1}$), putting them at the high-end of the linear size distribution. GRGs have been observed at both low and high frequencies to study their morphological character, magnetic field distribution and flux density. It is believed that the lobes of GRGs are moving outwards through the low-density (10^{-5} – 10^{-6} cm^{-3}) intergalactic medium (IGM), and their estimated spectral ages are about 10^7 – 10^8 years (Mack et al. 1998; Jamrozy et al. 2008).

DA 240 is a typical GRG with an intermediate value of radio luminosity which lies in the transition region between FR I and II types (Fanaroff & Riley 1974). It has two lobes with a prominent hotspot in the NE component and a weaker one to the SW. The angular size along the major axis of DA 240 is about 34 arcmin (measured from edge to edge) with a redshift of 0.0356 (Willis et al. 1974). Hence the linear size is 1.4 Mpc (for $H_0 = 71 \text{ km s}^{-1} \text{ Mpc}^{-1}$, $\Omega_m = 0.27$ and $\Omega_\Lambda = 0.73$).

In order to investigate the surrounding environment of DA 240, Peng et al. (2004)¹ obtained optical spectra and found that 16 galaxies had similar redshifts to the host galaxy of DA 240 (redshift of 0.0358), and that 10 of the 16 galaxies were distributed along the major axis of the radio emission. Moreover,

there may be a linear correlation between the relative velocity and projected distance along the source axis.

Here we report on our on-going research on faint galaxies around DA 240. A couple of new members can be added from published results of other research groups. We present our observations and data reduction in Sect. 2, the results and analysis in Sect. 3, a discussion in Sect. 4, and the conclusions in Sect. 5.

2. Observations and data reduction

2.1. Observations

In Paper I, there were four faint candidates for which we were unable to secure redshifts. These galaxies (listed in Table 1) are the subject of this article. In Table 1, we use the source numbers from Paper I. Columns 2–4 are the Right Ascension, Declination (J2000) and apparent *R*-band magnitude from the USNO-2.0 catalogue.

Following Paper I, we have made spectroscopic observations with the 2.16 m optical telescope and OMR spectrograph of Xinglong Station, NAOC, with a Tektronix 1024 × 1024 CCD as a detector for the first three candidates (Nos. 29, 30, 31). We used the grism of 300 g mm⁻¹ with wavelength coverage of 3800–8000 Å. The slit width was 2'' arc and the average spectral resolution was about 9.6 Å. Exposures of 3600–7200 s were taken on the night of January 29th, 2003. For candidate No. 32, we used

¹ Hereafter called Paper I.

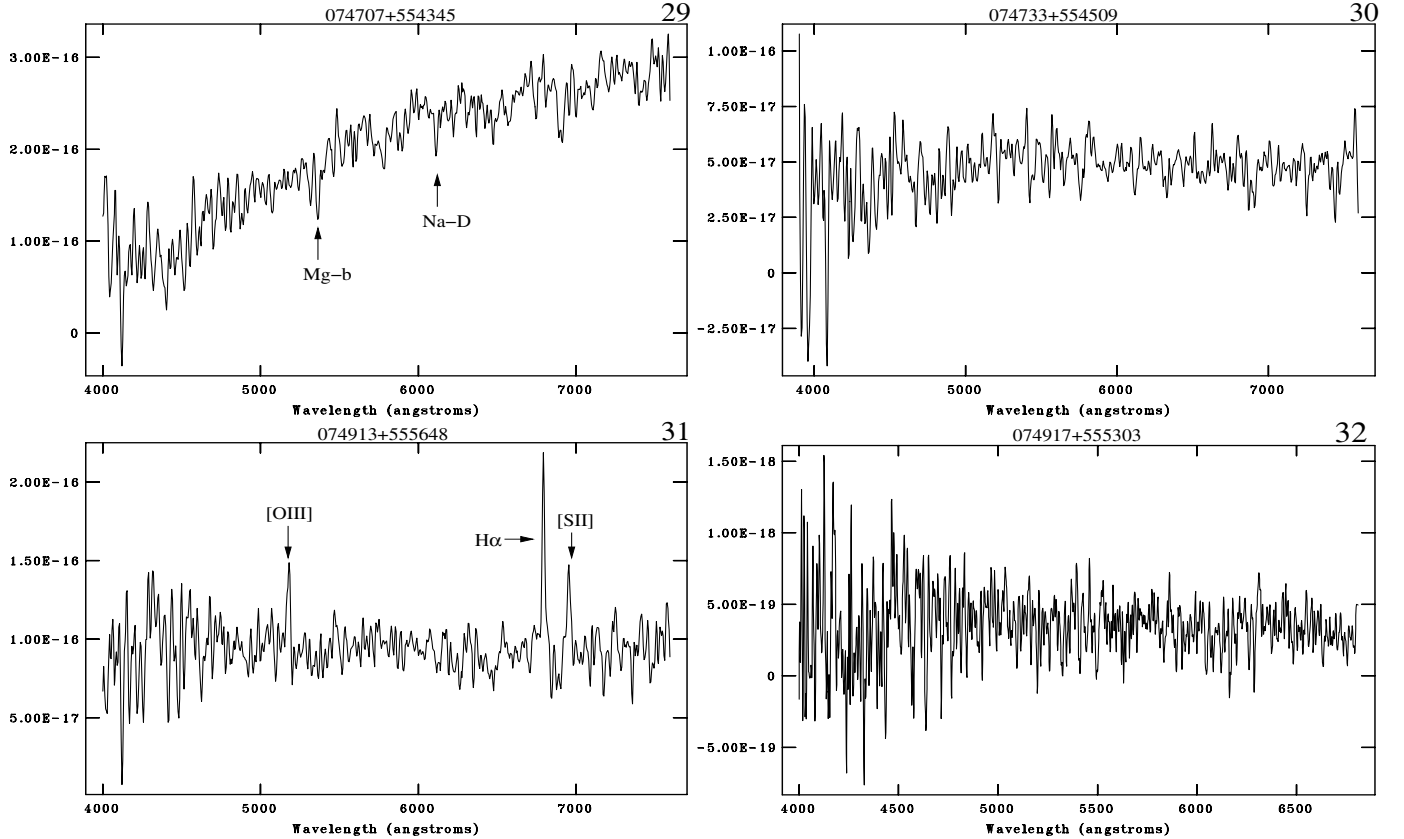


Fig. 1. Spectra of the four galaxies around DA 240, observed with the 2.16 m optical telescope at Xinglong Station of the NAOC (wavelength not corrected for redshift). The identified lines are marked.

Table 1. Four candidate galaxies from Paper I.

No.	RA (J2000) h m s	Dec (J2000) ° ' "	<i>R</i> app. mag
29	07 47 07.51	55 43 45.5	15.7
30	07 47 33.70	55 45 09.0	16.8
31	07 49 13.49	55 56 48.5	17.5
32	07 49 17.14	55 53 03.1	17.9

the BFOSC² spectrograph with a Tektronix 2048 × 2048 CCD as a detector. We used grism G7, for which the reciprocal dispersion is 95 Å/mm with wavelength coverage of 3870–6760 Å. The slit width was 1.8'' arc and the average spectral resolution was about 1.4 Å. Exposures of 10 800 s were taken on the night of January 6th, 2010. As galaxies are not point sources, the magnitudes given are just indicative values, especially for those with large envelopes. Galaxies with the same indicative magnitude may appear to differ by a lot in an observation. Although we made several attempts, the 32nd candidate of 17.9 mag in the *R* band was too faint for the OMR spectrograph. It was difficult to align this faint galaxy with the slit and the S/N was too low. So we decided to use the BFOSC spectrograph as the detector and took an exposure of three hours. We used helium and argon lamps for the OMR, and Ferrum and argon lamps for the BFOSC to facilitate wavelength calibration. The flux calibration was done by exposures of KPNO standard stars (Massey et al. 1988), such as HD 19445 and G191B2B. The atmospheric extinction was corrected by the mean value for Xinglong. However,

² BAO Faint Object Spectrograph and Camera.

we did not remove the telluric O₂ absorption bands at 6870 Å and 7620 Å.

2.2. Data reduction

The optical data was reduced with IRAF³ software. After wavelength and flux calibration, we inspected the absorption and emission features of each spectrum. The redshifts were calculated after the identification of several spectral lines, and the average value and its error were finally derived. The reduced spectra are shown in Fig. 1, and their redshifts are listed in Col. 4 of Table 2. Unfortunately, there are no lines in the spectra of Nos. 30 and 32. For this reason no redshift could be determined.

We also made simple classifications for the four objects following the criteria of Veilleux & Osterbrock (1987). Galaxies without emission lines are classified as normal (G), while objects with H_α emission line but weak forbidden lines of [NII] 6583 Å and [OIII] 5007 Å are classified as HII.

The radio data are from observations made by the Westerbork Synthesis Radio Telescope (WSRT) at a frequency of 608 MHz, which consisted of two 12 h observations with 36 and 72 m settings of the shortest baseline. The final cleaned radio map was provided by one of us (BP), and some analysis was done using AIPS⁴ software.

3. Results and analysis

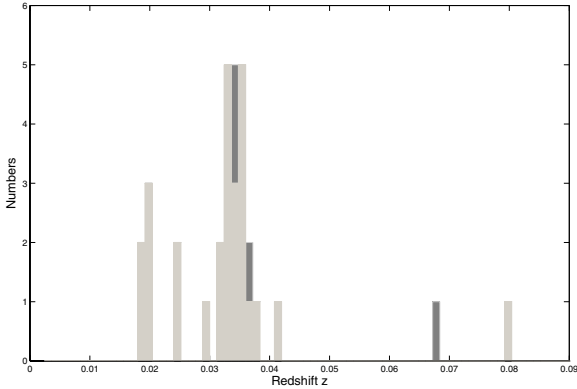
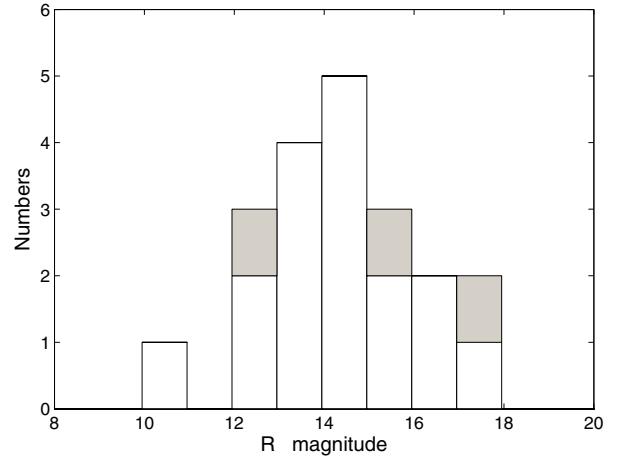
We have obtained spectra of four additional galaxies around DA 240 which had not been observed for Paper I and are listed

³ Image Reduction and Analysis Facility.

⁴ Astronomical Image Processing System.

Table 2. Summary of the observing results: four galaxies observed with the 2.16 m optical telescope.

No.	RA+Dec name (J2000)	Obs. dates yyyy.mm.dd	Redshift z	Exposure s	Notes	C
29	074707.51+554345.5	2003.01.29	0.0367 ± 0.0003	3600	Na-D, Mg-b	G
30	074733.70+554509.0	2003.01.29	–	7200	(no features detected)	G?
31	074913.49+555648.5	2003.01.29	0.0347 ± 0.0005	3600	H α , [SII], [OIII]	HII
32	074917.14+555303.1	2010.01.06	–	10800	(no features detected)	G?


Fig. 2. Histogram of the redshift distribution for the 31 galaxies in the direction of DA 240. The four new redshifts are shown in dark shading, while Nos. 18 (0.1237) and 35 (0.174) are beyond the region plotted.

Fig. 3. Magnitude distribution of the 20 galaxies in the main group. The additional three members are shown with a darker shade.

in Table 2. Column 1 is the source number and Col. 2 is the coordinate name. Columns 3–5 are the observation dates, redshifts, and exposure times. Column 6 lists the line identifications, and the last column is the classification of galaxy type.

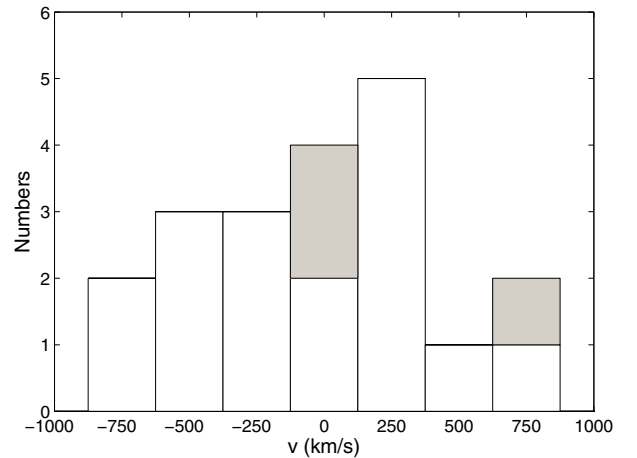
In addition to the four candidates we have observed, the redshifts of other three galaxies recently became available on the NASA/IPAC Extragalactic Database (NED). They are $z = 0.034207$ (Rines et al. 2000), 0.067296 (Rines et al. 2004) and 0.174 (Stoche et al. 1991). They have been added to our sample, labelled Nos. 33, 34 and 35 respectively, and are included in the discussion below.

3.1. Redshifts and magnitude

We have put all the results for the 33 candidates together⁵, and readily find that three new galaxies can be added to the DA 240 main group with $0.032 \leq z \leq 0.038$, as can be seen in a histogram (Fig. 2). The two other galaxies we observed (Table 2) are probably background objects, although their redshifts remain unknown. In any event, the main group now has 20 galaxy members. Figure 3 is the red magnitude distribution of these 20 members, with the host galaxy conspicuously brighter than the rest. This is evidence that the DA 240 host galaxy is the dominant member in terms of stellar mass.

3.2. Velocity distribution

We have inspected the velocity distribution of the group members. We take the velocity of galaxy No. 9 (in Paper I we used galaxy No. 6) as our reference point, as it is closest to the median value. From Fig. 4, we find a noticeable peak at about 250 km s^{-1}


Fig. 4. Velocity distribution of the 20 group members. The additional three are shown with dark shading.

in the velocity distribution. Comparing it with a Gaussian distribution of the same mean v and σ , a χ^2 test indicates that the probability of the velocities being normally distributed is about 32% (15% in Paper I): the distribution does not differ significantly from a Gaussian.

3.3. Locations and dynamic lifetime

The locations of the 20 main group galaxies are illustrated together with the 49 cm radio brightness distribution in Fig. 5. The three additional galaxies are displayed with different symbols. Two are in one lobe while one is in the other: galaxy Nos. 31, 33 are in the NE lobe while galaxy No. 29 lies in the SW

⁵ The redshifts and coordinates of all 33 galaxies are listed in Appendix Table A.1.

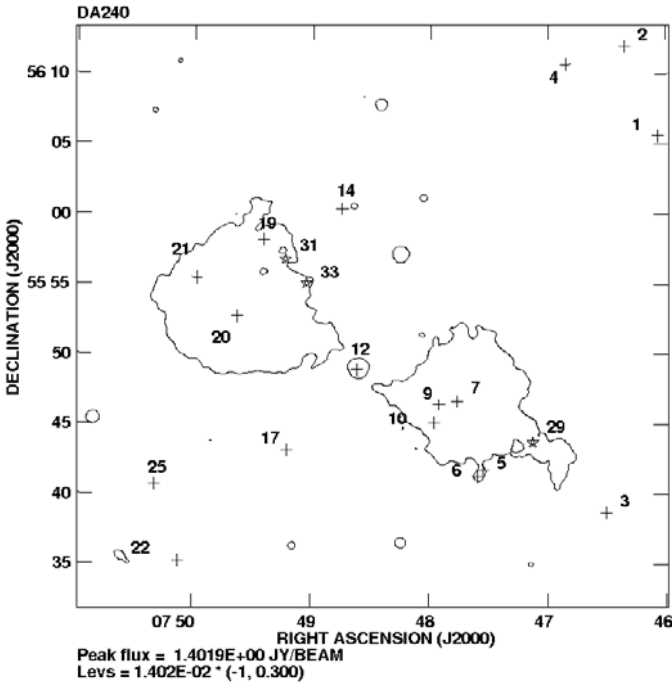


Fig. 5. DA 240 single-contour map (showing the radio extent) obtained with the WSRT at 49 cm, with 20 optical galaxies at redshifts $0.032 \leq z \leq 0.038$. The previous 17 members are plotted with crosses while the three additions (Nos. 29, 31 and 33) are with stars.

one. So, there are six galaxies (including galaxy No. 14) around the NE lobe and seven around the SW lobe (including No. 3). Another striking feature of the galaxy distribution is the absence of any close companions to VV 9-13-57 (the DA 240 host). The nearest group member is galaxy No. 9, at a projected distance of some 250 kpc from VV 9-13-57. We will return to this point in Sect. 4 below.

We can compute the dynamic lifetime of each galaxy group to compare it with the radiation age of the respective lobe as was done in Paper I. Since one can only measure the line-of-sight velocity, we have corrected the velocity dispersions to account for this. For the eastern group, the dispersion is, $\sigma = 478 \text{ km s}^{-1}$, and 766 km s^{-1} for the western group. Considering the lobe radii are both about 400 kpc, it is straightforward to derive dynamic lifetimes of $8 \times 10^8 \text{ yr}$ for eastern group and $5 \times 10^8 \text{ yr}$ for western group. We quoted a value for the radiation age in Paper I, which was $t \leq 10^7 \text{ yr}$. Hence the kinematic lifetime of the galaxy groups is comfortably larger than the radiation age of the radio lobes.

3.4. Monte-Carlo simulation

There are now 13 galaxies (excluding No. 14) lying along the major axis as defined by the radio core and hotspots of DA 240. In order to test whether the alignment of the 13 members is significant, a Monte-Carlo simulation has been performed. The lobes are constrained by two lines passing through galaxy No. 12 (VV 9-13-57), 19° on each side of the major axis. With 13 galaxies in this defined area, we computed the probability of 13 or more appearing there by chance. Locations of the 20 members were randomly generated, and the process was repeated 10^7 times. This experiment showed that the configuration observed would happen by chance at a rate of 7×10^{-6} , compared

with the value of 3×10^{-4} in Paper I, where the number of group members was 17 and only 10 appeared in the same constrained area. The three additional galaxies strengthen the case that the alignment is physically significant.

3.5. Relative distance and velocity

We have also looked into the kinematics of the 14 galaxies lying in or near the radio lobes. After projecting locations of the galaxies onto the radio axis, we have computed their projected distance from galaxy No. 12. In this way we have generated an updated version (not shown) of Fig. 7 which appeared in Paper I. We find that there is still a correlation between Δv and D , although the correlation coefficient has decreased to -0.67 from the -0.74 of Paper I. And after a least-squares fit to those points, the gradient is -0.391 (up from -0.425 in Paper I), indicating $\Delta v/D = 391 \text{ km s}^{-1} \text{ Mpc}^{-1}$. We can also compute the enclosed mass for the case of galaxies seen in an edge-on ring, orbiting the center. For $d/2 = r \approx 1 \text{ Mpc}$ and $v_{\text{orb}} \approx 391 \text{ km s}^{-1}$, the mass is $M = rv_{\text{orb}}^2/G = 3.5 \times 10^{13} M_{\odot}$.

4. Discussion

We begin by considering the larger-scale environment in which the DA 240 group is embedded. As already noted in Paper I, DA 240 lies on the western edge of the Zwicky cluster Zw 0756.1+5616 (Zwicky & Herzog 1966). Almost 4° to the west lies another large cluster, Abell 576, at a somewhat greater distance ($z \approx 0.039$) than DA 240. Optical information on A576 can be found in the catalogue of Hudson et al. (2001). After the publication of Paper I, the NOAO Fundamental Plane Survey appeared (Smith et al. 2004). It includes redshift information on the UGC 3957 galaxy group. UGC 3957 lies between DA 240 and A576, at a redshift of $z = 0.034$. It consists of more galaxies (over 50 spectroscopically confirmed and listed in NED) than the DA 240 group, but has a similar diameter and only a slightly smaller redshift. The two may form a binary system, a not uncommon phenomenon (Karachentsev & Kopylov 1981; Karachentsev & Shcherbanovskii 1978; and Ulmer et al. 1985). However, they appear to be well-separated both spatially (Fig. 6) and in distance (cz differs by 170 km s^{-1} , or 2.3 Mpc), and may be too remote from one another (total separation of $\sim 3.4 \text{ Mpc}$ if the velocity difference is purely due to Hubble expansion, although this is not necessarily the case if the two groups are interacting dynamically) to be considered a true binary.

In Fig. 6, we show the locations of all galaxies within a radius of 8° from the DA 240 host and in the redshift range of the group, $0.032 \leq z \leq 0.038$. The two central concentrations are the UGC 3957 and DA 240 galaxy groups. To the west and slightly north, we have A576. Its central condensation is clearly visible, despite the fact that the $z \leq 0.038$ upper limit means that only about half of the galaxies in the cluster are shown in this figure. Most of the galaxies to the east belong to Zw 0756.1+5616. The limit of the SDSS region runs through the center of the figure near $RA = 8^{\text{h}}$; the spectra of many of the galaxies east of this line come from the SDSS. Figure 7 shows the distribution in redshift for galaxies in four regions of sky centered on the two groups, and the Abell and Zwicky clusters. These histograms clearly show that A576 has a somewhat higher average redshift than the groups and Zw 0756.1+5616, though there is significant overlap in the lower- z wing. The DA 240 and UGC 3957 groups, and the Zwicky cluster, overlap considerably in redshift, though they are spatially distinct.

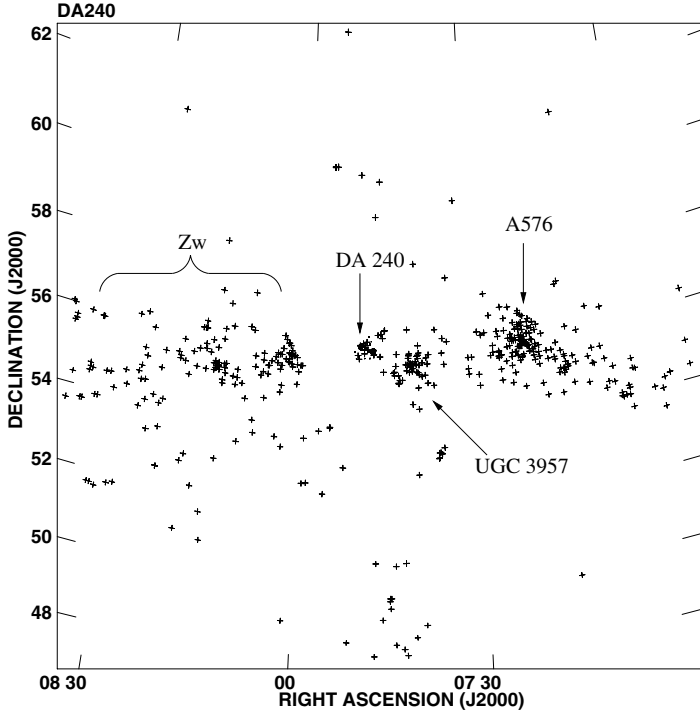


Fig. 6. Locations of all galaxies within a radius of 8° from the DA 240 host and in the redshift range of $0.032 \leq z \leq 0.038$. Rough locations of the four clusters/groups are indicated, where Zw stands for the Zwicky cluster Zw 0756.1+5616.

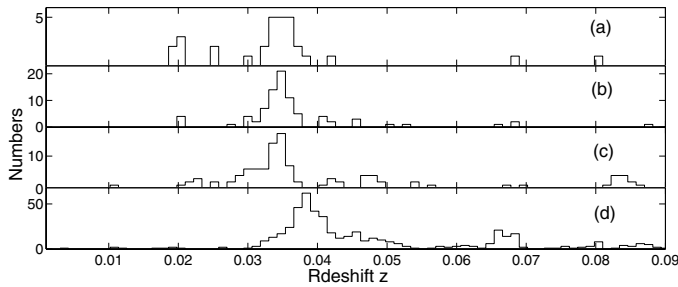


Fig. 7. Redshift distributions of four groups: **a)** DA 240; **b)** UGC 3957; **c)** Zw 0756.1+5616; **d)** Abell 576.

In Fig. 8 we show, for all galaxies in the same region of space as Fig. 6, but over the redshift range $0.02 \leq z \leq 0.05$, a plot of RA vs. cz . A576 is clearly seen near $RA = 7.4^h$, $cz = 11\,500 \text{ km s}^{-1}$. There appears to be a filament from A576, going to higher RA and higher v . From an examination of the RA, Dec, velocity cube (not shown), we conclude that this feature has a nearly constant Dec. Zw 0756.1+5616 is not as concentrated as A576, and most of its members fall in the range, $8^h \leq RA \leq 8.6^h$. The DA 240 and UGC 3957 groups fall in a gap between the Abell and Zwicky clusters. Although there are clearly fewer galaxies east and west of the two groups, one might wonder whether the gaps are related to the border of the SDSS survey region. We would argue that this should equally affect the higher-velocity filament (Fig. 8), yet it is almost continuous (there is a slight deficiency of galaxies near $RA = 7.75^h$, without the same gaps that isolate the DA 240 and UGC 3957 groups). We conclude that although there are other associations in the (both spatial and velocity) neighborhood, the two small groups form a separate structure, possibly a binary in which the UGC 3957 group dominates. Binary galaxy clusters may be in

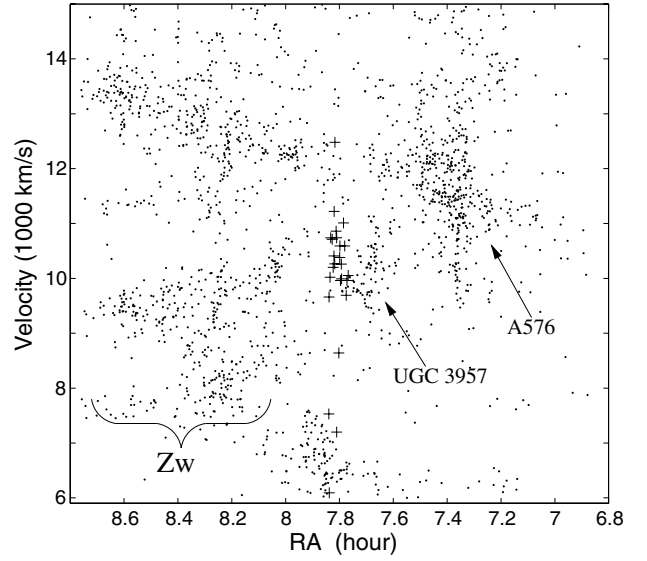


Fig. 8. Velocity vs. Right Ascension. Galaxies in the DA 240 sample are marked with crosses. The other group and two clusters are indicated using the same symbols as in Fig. 6.

the process of merging and this could trigger activity in their constituent galaxy members (Hwang & Lee 2009). As we have noted before (Peng et al. 2004), there is an excess of active galaxies in the DA 240 group.

What is the environment of other GRGs? Recent work on two southern sources can help put things in a broader context. MSH 05–22 and MRC B0319–454 are somewhat larger than DA 240; morphologically, they are fairly typical of GRGs, with collimated lobes which decrease in brightness with increasing distance from the head. Jet structures are observed in both sources, and the relative lobe length is quite unequal, which is not the case for DA 240. In a study of MSH 05–22, Subrahmanyam et al. (2008) find that the source is located 1–2 Mpc south of the center of the group of which the host is a member. This group is on the edge of a higher-density concentration in the form of a sheet or filament. The southern radio lobe is some 60% longer than its northern counterpart; the latter is also displaced laterally with respect to the host location. A possible explanation for the differences in lobe structure is a wind flowing out from the galaxy concentration to the northeast, and both displacing and retarding the northern radio lobe.

MRC B0319–454 shares some of the characteristics of MSH 05–22, but there are also differences (Safouris et al. 2009). Both are associated with small galaxy groups on the periphery of larger conglomerations. In MRC B0319–454, the more distant lobe leading edge, which ends in a bright hotspot, is over twice as far from the host as its counterpart to the northeast. The host has half a dozen companions which form a small group around the (shorter) northeastern lobe, while most of the galaxies of similar redshift are scattered to the southwest and west. The southwestern component trails off from the hotspot almost perpendicular to the source major axis. A plausible explanation for this behavior can be found in buoyancy of the jet backflow (Safouris et al. 2009). DA 240 is different from these two sources in several respects. In terms of the radio morphology, its lobes are much more symmetrical, both contain hotspots (though of very different intensity) and the low surface brightness morphology is roughly circular (though the western lobe

has a “tongue” of emission leading its hotspot). The galaxies in the DA 240 group are rather symmetric about the host, with a majority lying along the radio source axis. One thing all three radio sources share is that they are associated with small groups on the edge of much larger galaxy clusters.

Let us now try to put some of our results into the context of what is more generally known about medium-sized groups of galaxies, of which both the UGC 3957 and DA 240 groups are evident examples. Tully (1987) has collected a sample of well over 100 groups and other associations based upon surveys, for $cz < 3000 \text{ km s}^{-1}$. He has taken great care in defining what constitutes an association in his sample. The most relevant subset are the 49 groups with five or more members, which Tully has extensively investigated. He presents information on the collective fundamental physical properties of his sample, which can be used as a benchmark for the DA 240 group. He finds, for example, that the distribution of galaxy velocities about the mean is symmetrical, just as we see (Fig. 4). The mean velocity dispersion in his sample, however, is 100 km s^{-1} , considerably lower than the 434 km s^{-1} of the DA 240 group, though similar to that of UGC 3957.

Various studies have shown that there are correlations between the velocity dispersions of clusters of galaxies and the temperature and X-ray luminosity of their hot gas. Mulchaey & Zabludoff (1998), for example, show that the X-ray temperature and velocity dispersion of groups are correlated and form an extension of the correlation found for clusters. A similar relationship is found between velocity dispersion and X-ray luminosity, with again groups falling on an extension of the cluster correlation. Attempts to detect X-ray emission from DA 240 and its surroundings have been only partially successful. Miller et al. (1999) used the *ROSAT* All Sky Survey data to set a limit to the DA 240 X-ray luminosity of about $10^{42} \text{ erg s}^{-1}$. Evans et al. (2008) used *XMM-Newton* to detect X-rays from VV 9-13-57 at a level of $5.5 \times 10^{40} \text{ erg s}^{-1}$. This unresolved emission originates, they conclude, in the parsec-scale jet in the galaxy’s nucleus. They also present an X-ray map of the entire GRG showing no trace of extended emission, confirming the Miller et al. (1999) upper limit.

It is a bit surprising to find no X-ray emission from the center of the DA 240 group, given its substantial velocity dispersion. According to the correlations found by Mulchaey & Zabludoff (1998), the group might be expected to have an X-ray luminosity of $10^{43} \text{ erg s}^{-1}$ with a gas temperature slightly in excess of 1 keV, although there is significant scatter in the data. There are at least two other unusual facts about the DA 240 group. The galaxies in poor groups are almost always concentrated toward the center (see Beers et al. 1995, for numerous examples; this is, of course, also true of clusters). In the case of the DA 240 group, there is a conspicuous absence of galaxies in the vicinity of VV 9-13-57. As noted above, its nearest neighbor is No. 9, at a projected distance of 250 kpc. The fact that VV 9-13-57 lies at the geometrical center of the group is as expected (Beers et al. 1995), but unusually, kinematically, the galaxy is offset by $+370 \text{ km s}^{-1}$ from the group average, 10360 km s^{-1} . Beers et al. (1995) find that in 80% of the poor clusters they studied, the central galaxies show relatively small velocity offsets.

We have, at the moment, no explanation for the lack of a hot, substantially dense gaseous component, nor for the absence of galaxies near the center of the group. Perhaps it is somehow related to the binary nature of the group, if it is still in the process of merging. We note that both a lower ambient density and the absence of nearby companions are both consistent with the presence of a GRG, and one with broad components which have

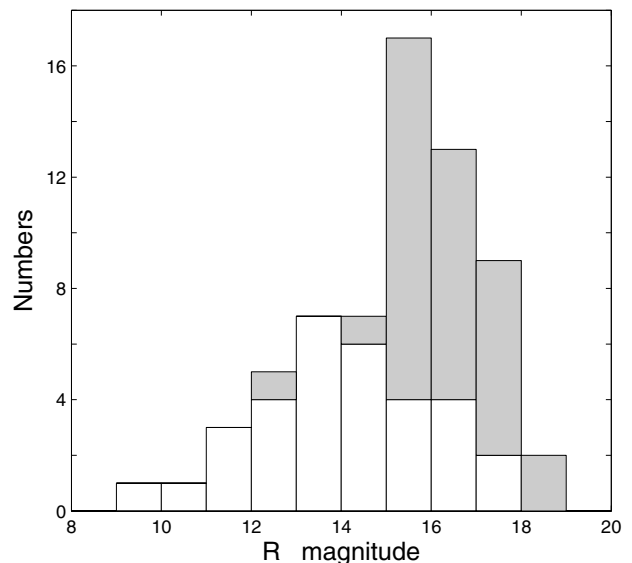


Fig. 9. A histogram showing the R-magnitudes of the galaxies we have studied (Table A.1) traced with a solid line, and in shading the magnitudes of the remaining USNO galaxies.

expanded laterally almost as far as they have moved away from the host.

5. Conclusions

Apart from the two faint members (Nos. 30 and 32) we have essentially completed our spectral investigation of galaxies within $30'$ arc of DA 240. We have redshifts for 33 galaxies on our original list. There is, to be sure, roughly an equal number of additional galaxies in the same region of sky from the USNO catalogue, but they are fainter than most of the galaxies in our original sample. The R-band magnitudes for these uninvestigated objects are compared with those from the sample of 33 in Fig. 9, showing that they are mainly on the faint side of the distribution. There remains one fairly bright ($R = 12^m$) galaxy, J075150+554119 from the USNO A2 list; it is at the extreme SE end of our search zone.

Apart from J075150+554119, our investigation of the DA 240 group is practically complete for all galaxies with $R < 15^m$ within 1.2 Mpc of the radio source host. Since there may be fainter members of the group, our conclusions apply to the brighter, dominant galaxies.

In this paper, we have added three candidates to the confirmed members of the DA 240 group. All three of these galaxies lie near the lobes, increasing the number of galaxies lying along the radio major axis from 11 to 14. This strengthens the case for alignment not having arisen by chance, as shown by our Monte-Carlo simulation. The kinematic timescale for group members which cluster in or near the lobes is also clearly larger than the lobes’ radiation ages. Furthermore, as found in Paper I, there is a correlation between the relative projected distance and velocity.

Our work confirms the results of Paper I, though they still remain unexplained. We have also looked into the larger-scale environment around the DA 240 group, and find that it has a “sister” group of similar size, and that the two are not far from a substantial Abell cluster. The likelihood that the two groups may still be merging could affect activity of the individual galaxies. The absence of galaxies and dense gas within 250 kpc of the

host galaxy helps explain the huge size of the radio lobes: there is hardly anything to impede their expansion. To continue this investigation of the environments of GRGs, we are extending the study to other nearby sources.

Acknowledgements. We are grateful to the referee, Dr. D. J. Saikia, for a number of suggestions which have considerably improved the paper. This work was partially supported by the Open Project Program of the Key Laboratory of Optical Astronomy, NAOC, CAS. The Westerbork Synthesis Radio Telescope is operated by The Netherlands Institute for Radio Astronomy (ASTRON), with financial support from The Netherlands Organization for Scientific Research (NWO). We thank the Chinese and Royal Netherlands Academies of Sciences (CAS and KNAW) for financial support under a bilateral exchange programme which has facilitated travel by B.P. and R.G.S., R.G.S. is also grateful to the CAS for the award of a Visiting Professorship for Senior International Scientists. We also thank Dr. C. Jin and Dr. J. Wang for their help with the data reduction, and Dr. H. Wu for providing extra telescope time when weather curtailed an observing run. This research has made use of the NASA/ADS Abstract Service, and of NED which is operated by the Jet Propulsion Laboratory, Caltech, under contract with the National Aeronautics and Space Administration. We are grateful for the use of the USNO-A2.0 catalogue.

References

- Beers, T. C., Kriessler, J. R., Bird, C. M., & Huchra, J. P. 1995, *AJ*, 109, 874
 Evans, D. A., Hardcastle, M. J., Lee, J. C., et al. 2008, *ApJ*, 688, 844
 Fanaroff, B. L., & Riley, J. M. 1974, *MNRAS*, 167, L31
 Hudson, M. J., Lucey, J. R., Smith, R. J., Schlegel, D. J., & Davies, R. L. 2001, *MNRAS*, 327, 265
 Hwang, H. S., & Lee, M. G. 2009, *MNRAS*, 397, 2111
 Jamrozy, M., Konar, C., Machalski, J., & Saikia, D. J. 2008, *MNRAS*, 385, 1286
 Karachentsev, I. D., & Kopylov, A. I. 1981, *Sov. Astr. L.*, 7, 285
 Karachentsev, I. D., & Shcherbanovskii, A. L. 1978, *Sov. Astr.*, 22, 257
 Klein, U., Mack, K.-H., Strom, R. G., Wielebinski, R., & Achatz, U. 1994, *A&A*, 283, 729
 Mulchaey, J. S., & Zabludoff, A. I. 1998, *ApJ*, 496, 73
 Mack, K. H., Klein, U., O' Dea, C. P., Willis, A. G., & Saripalli, L. 1998, *A&A*, 329, 431
 Massey, P., Strobel, K., Barnes, J. V., & Anderson, E. 1988, *ApJ*, 328, 315
 Miller, N. A., Owen, F. N., Burns, J. O., Ledlow, M. J., & Voges, W. 1999, *AJ*, 118, 1988
 Lang, K. R. 1999, *Astrophysical Formulae*, 2 vols (Berlin: Springer-Verlag)
 Peng, B., Strom, R. G., Wei, J., & Zhao, Y. H. 2004, *A&A*, 415, 487
 Rines, K., Geller, M. J., Diaferio, A., Mohr, J. J., & Wegner G. A. 2000, *AJ*, 120, 2338
 Rines, K., Geller, M. J., Diaferio, A., Kurtz, M. J., & Jarrett, T. H. 2004, *AJ*, 128, 1078
 Safouris, V., Subrahmanyan, R., Bicknell, G. V., & Saripalli, L. 2009, *MNRAS*, 393, 2
 Smith, R. J., Hudson, M. J., Nelan, J. E., et al. 2004, *AJ*, 128, 1558
 Stocke, J. T., Morris, S. L., Gioia, I. M., et al. 1991, *ApJS*, 76, 813
 Subrahmanyan, R., Saripalli, L., Safouris, V., & Hunstead, R. W. 2008, *ApJ*, 677, 63
 Tully, R. B. 1987, *ApJ*, 321, 280
 Ulmer, M. P., Cruddace, R. G., & Kowalski, M. P. 1985, *ApJ*, 290, 551
 Veilleux, S., & Osterbrock, D. E. 1987, *ApJS*, 63, 295
 Willis, A. G., Strom, R. G., & Wilson, A. S. 1974, *Nature*, 250, 625
 Zwicky, F., & Herzog, E. 1966, *Catalogue of Galaxies and Clusters of Galaxies* (Pasadena: California Institute of Technology)

Appendix A

An overview of all the galaxies in our DA 240 sample is provided in Table A.1.

Table A.1. Thirty-three galaxies in the DA 240 sample.

No.	RA (J2000)			Dec (J2000)			<i>R</i> app. mag	<i>z</i>
	h	m	s	°	'	''		
1	07	46	03.94	56	05	36.2	13.1	0.0335
2	07	46	20.83	56	11	57.8	13.2	0.0332
3	07	46	30.26	55	38	44.2	14.6	0.0323
4	07	46	51.07	56	10	42.1	14.2	0.0353
5	07	47	32.90	55	41	48.2	16.5	0.0333
6	07	47	35.52	55	41	18.5	12.6	0.0342
7	07	47	45.94	55	46	41.4	17.2	0.0332
8	07	47	51.26	55	47	06.7	15.7	0.0800
9	07	47	55.12	55	46	28.3	13.9	0.0353
10	07	47	57.75	55	45	10.1	15.0	0.0346
11	07	48	08.29	55	48	15.5	14.1	0.0288
12	07	48	36.87	55	48	58.3	10.7	0.0358
13	07	48	36.87	55	48	58.3	16.4	0.024
14	07	48	44.76	56	00	35.5	16.8	0.0362
15	07	49	01.27	55	25	32.0	13.9	0.0416
16	07	49	09.84	55	36	16.8	11.4	0.0183
17	07	49	12.28	55	43	12.2	14.2	0.0374
18	07	49	12.62	55	52	33.6	14.7	0.1237
19	07	49	24.56	55	58	13.4	14.1	0.0340
20	07	49	37.90	55	52	44.4	14.3	0.0357
21	07	49	58.51	55	55	28.0	12.7	0.0358
22	07	50	07.12	55	35	14.5	13.2	0.0334
23	07	50	08.40	55	23	03.0	9.5	0.0193
24	07	50	16.36	55	24	29.9	11.0	0.0203
25	07	50	19.34	55	40	41.5	15.0	0.0322
26	07	50	21.33	55	54	01.4	11.7	0.0251
27	07	50	28.99	55	29	01.8	13.0	0.0190
28	07	50	53.10	55	27	58.1	12.8	0.0196
29	07	47	07.51	55	43	45.5	15.7	0.0367
31	07	49	13.49	55	56	48.5	17.5	0.0347
33	07	49	02.7	55	55	07	12.2	0.034207
34	07	45	27.5	55	47	28	13.9	0.067296
35	07	49	09.3	55	37	55	16.6	0.1740